Chapter 2

Probing coiled-coil assembly by paramagnetic NMR spectroscopy

Zheng, T. T.; Boyle A.; Marsden, H. R.; Raap, J.; Valdink, D.; Martelli, G.; Kros, A., Probing coiled-coil assembly by paramagnetic NMR spectroscopy. Organic & biomolecular chemistry. 2014, Accepted.

Abstract

Here a new method to monitor the aggregation process and orientation of coiled coil peptide motifs is described. Peptides Coil-K and Coil-E which are designed to form a heterodimeric complex were labeled with aromatic FRET pair tryptophan (W) and tyrosine (Y) on the C-terminus respectively as a 'fingerprint' residue. One of the peptides was also labeled with the paramagnetic probe MTSL. Circular dichroism spectroscopy confirmed that the introduction of the MTSL label did not change the peptide secondary structure. One dimensional (1D)-proton NMR spectroscopy was used to study the peptide quaternary structure by monitoring the fluorophore aromatic NMR signal suppression due to proximity of the nitroxyl radical MTSL. 1D-NMR confirmed that peptide Coil-K and Coil-E form a heterodimer coiled coil with a parallel orientation. In addition, fluorescence emission quenching of the aromatic residue due to electron exchange with a nitroxyl radical confirmed the parallel coiled coil orientation. Thus, paramagnetic nitroxide and aromatic fluorophore labeling of peptides yield valuable information on the quaternary structure from 1D-NMR and steady-state fluorescence measurements. This convenient method is useful not only to investigate coiled coil assembly, but can also be applied to other supramolecular assemblies or biomacromolecules with a defined structure.

Introduction

Coiled coils are a structural motif comprised of two to seven α-helices folding around each other in a superhelical fashion and are one of the important subunit motifs found in proteins.[1-8] In nature, this versatile protein folding motif assembles in a wide range of structures with a variety of functions.[9] One of the well-known coiled coil motifs are the so-called SNARE proteins, which is at center of the highly controlled intracellular membrane fusion mechanism enabling cell-to-cell communication in the nervous system.[10, 11] Recently, a model system for in vitro membrane fusion, mimicking the SNARE protein complex has been designed.[12-15] Here, membrane fusion was achieved by a pair of complementary lipidated peptides comprised of the heterodimeric coiled coil pair CC-K/E.[16] However, the details of the fusion mechanism are still unclear. To obtain a better view on the membrane fusion mechanism, the coiled coil peptide CC-K/E quaternary structure has been studied. Typically X-ray diffraction, disulfide exchange, electron paramagnetic resonance (EPR),

two-dimensional nuclear magnetic resonance (2D-NMR), 3D-NMR and even 4D-NMR techniques are employed to study the architecture of coiled coil peptide quaternary structures, for example the number of peptides in an assembly, the stoichiometry and their relative orientation.[17-28] However most of these techniques require expensive and complex equipment, which is not always readily available. Therefore, it is valuable to develop simple method that only requires standard laboratory equipment.

Here, a simple and easy method to investigate the coiled coil peptide assembly and orientation with a simple one-dimensional proton nuclear magnetic resonance (^{1}H-NMR) and steady state fluorescence measurements is reported.

To demonstrate our approach, the well-known E/K motif developed by Litowsky and Hodges was used as a model system. In recent years this coiled coil has been used by several groups in the field of supramolecular chemistry, polymers and membrane fusion.[29-35] The coiled coil peptides Coil-K (Ac-$(KIAALKE)_3$-$CONH_2$) and Coil-E (Ac-$(EIAALEK)_3$-$CONH_2$) were labeled with tryptophan (W) and tyrosine (Y) at the C-terminus as a fluorophore FRET (fluorescence resonance energy transfer) pair respectively. Furthermore, the aromatic signals in 1D-proton NMR spectra are well-separated from all other proton signals. This allows for easy paramagnetic NMR spectroscopy analysis to determine the peptide orientation within the coiled coil motif. According to their characteristics in ^{1}H-NMR and fluorescence measurements, W and Y are defined as the 'fingerprint' functional group of peptide Coil-K and Coil-E respectively.

In this study, the paramagnetic nitroxyl radical MTSL (S-(2,2,5,5-tetramethyl-2,5-dihydro-1H-pyrrol-3-yl)methyl methanesulfonothioate) (see Appendix Part 6 for its chemical structure) was introduced at specific positions in the peptide to investigate the coiled coil assembly and peptide orientation.[36, 37] In ^{1}H-NMR, there are magnetic dipolar interactions if the distance between a nucleus and an unpaired electron of a paramagnetic center is within 13.0 Å radius, leading to paramagnetic relaxation enhancement (PRE).[38-43] This increases the relaxation rate of the nuclear magnetization, and results in the suppression of the nucleus NMR signal.[40, 44] As a result, the neighboring signal will be drastically suppressed when it is located within 10.5 Å of the spin label. For example, in a 1D-proton NMR experiment, the proton signals of W or Y will be significantly suppressed when they are in proximity of the paramagnetic MTSL probe. In addition, the fluorescence will also be quenched by the intermolecular electron-exchange interaction between the ground-state stable nitroxide (MTSL) radical and the excited singlet state aromatic fluorophore (W and

Y) when the distance is less than 12 Å.[45-49] Thus in both NMR and fluorescence measurements, the proximity of a MTSL probe leads to signal suppression (See Appendix Figure A11 for the summary of the signal response regions from various measurements).

An equimolar mixture of Coil-K and Coil-E peptide results in the formation of a heterodimeric coiled coil motif CC-K/E. Both C-termini will be in close proximity when a parallel orientation is adopted; but will be on opposite sides of the coiled coil when an antiparallel orientation is adopted (Scheme 1.).

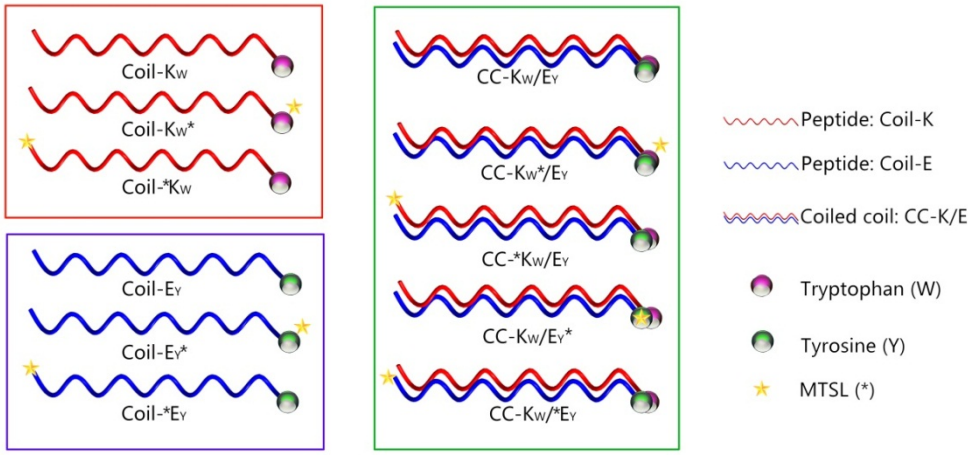

Scheme 1. Schematic illustration of designed peptides and coiled coil motifs. Coil-K peptides are labeled with a tryptophan(W) residue while Coil-E peptide are decorated with a tyrosine(Y) residue. A red helix represents peptide Coil-K, while a blue helix represents peptide Coil-E. Purple ball stands for tryptophan (W) labeled while green ball stands for tyrosine (Y) labeled. In this paper W and Y are always decorated on the C-terminus of all the peptides. A yellow star represents the MTSL- (*) nitroxyl radical spin label, which labeled either on C- or on N- terminus for investigating the possibility of CC-K/E parallel and antiparallel orientation respectively. Coiled coils formed by equimolar mixing of various Coil-K and Coil-E peptides are defined as CC-K/E. (See Table 1. for primary sequences of all peptides.)

The paramagnetic 1D-proton NMR and steady state fluorescence study demonstrates that the peptide Coil-K and Coil-E are forming a parallel heterodimeric coiled coil CC-K/E in neutral PBS buffer (Phosphate Buffer Saline). This is the first time that a paramagnetic nitroxide moiety is used to determine unequivocally the orientation and assembly of peptide strands in a coiled coil motif. Furthermore the peptide assembly ratio can be determined within a hetero-coiled coil complex. This method does not disturb self-

assembly and can be used to more complicate coiled coil motifs and allows broader applications in biomaterials field.

Experimental Section

Materials.

Fmoc-protected amino acids and Rink Amide resin (0.53 mmol g^{-1}) were purchased from NovaBiochem. HCTU (O-(1H-6-Chlorobenzotriazole-1-yl)-1,1,2,2-tetramethyluronium hexafluorophosphate), HOBT (1-Hydroxybenzotriazole) and DIPEA (N,N-Diisopropylethylamine) were from IRIS Biotech GmbH. NMP (N-methyl-2-pyrrolidone) and DMF (N,N-dimethylformamide) were from Biosolve. DCM (dichloromethane), TFE (2,2,2-Trifluoroethanol), TFE-D_3 (2,2,2-Trifluoroethanol-d_3), and deuterium oxide were obtained from Sigma-Aldrich. Acetic anhydride, piperidine, MeCN (acetonitrile), TFA (trifluoroacetic acid), and TIS (triisopropylsilane) were obtained from Fluka Chemie GmbH. MTSL ((S-(2,2,5,5-tetramethyl-2,5-dihydro-1H-pyrrol-3-yl)methyl methanesulfonothioate) was obtained from Toronto Research Chemicals Inc. PBS buffer contains: 30 mM K_2HPO4, 19 mM KH_2PO4, 150 mM NaCl, pH=7.4. The pH value was adjusted with either 0.1 M HCl or 0.1 M NaOH. Tris buffer contains 1M tris (2-Amino-2-hydroxymethyl-propane-1,3-diol), pH=7.0.

Peptide Synthesis.

Solid-phase peptide synthesis.

Peptides were synthesized on a CEM-Liberty 1 Single Channel Microwave Peptide Synthesizer using standard Fmoc chemistry.[50] Fmoc-protected Rink amide resin (0.53 mmol g^{-1}) was used to synthesize the peptides on a 0.25 mmol scale. The resin was swollen in DMF for 30 mins before use. Fmoc deprotection was performed using 20% (v/v) piperidine in DMF for 3 mins at 50 W with a maximum temperature of 80 ℃. Four equivalents of a Fmoc-amino acid, four equivalents of HCTU and five equivalents of DIPEA in DMF were used for amino acid coupling for 5 mins at 40 W with a maximum temperature of 80 ℃. For each amino acid coupling cycle, a deprotection and coupling time of 5 and 30 mins were used respectively. For cysteine coupling a cycle comprising 2

mins at 0 W followed by 4 mins at 40 W with a maximum temperature of 50 ^{o}C was used. Two wash steps (1.5 mL DMF) were performed between every amino acid coupling cycle. All peptides were acetylated manually at the N-terminus after completion of the synthesis using 20% (v/v) acetic anhydride in DMF for 1.5 hour. Peptides without a cysteine residue, were cleaved from the resin and side-chain deprotected using a mixture of TFA/water/TIS=95:2.5:2.5 (v/v) for 1 hour.[51] Peptides with a Trt (trityl-) protected cysteine residue were cleaved from the resin with simultaneous side-chain deprotection using TFA/thioanisole/ethandithiol/phenol/H_2O=8.4:0.7:0.5:0.2:0.2 (v/v) for 3 hours at room temperature.[52] The resulting solution was added drop-wise into an excess of 50ml cold diethyl ether to precipitate the deprotected peptide, followed by centrifugation and the liquid supernatant was removed. This procedure was repeated 3 times with the addition of fresh cold diethyl ether. All the peptides were dried under vacuum, dissolved in MilliQ water and lyophilized yielding a white powder.

MTSL nitroxyl radical label.

MTSL was conjugated to the peptide via a disulfide bond with the cysteine residue. One equivalent peptide (1 mM) was dissolved in 1 M tris buffer (pH=7.0) and five equivalents of MTSL in DMF (50 mM) were added slowly under an argon atmosphere and the final mixture was stirred for 3 hours at room temperature.[53] Next, the samples were lyophilized and stored at -20 ℃ before purification.

Peptide Purification.

The crude peptides were purified by RP-HPLC, using a Shimadzu HPLC system with two LC-8A pumps, and an SPD-10A VP UV-VIS detector. Samples elution was monitored by UV detection at 214 nm and 254 nm. Purification of peptides was performed on a Vydac C18 reversed phase preparative column with a flow rate 15 mL min^{-1}. Peptides were dissolved at a concentration of 5 mg ml^{-1} in a mixture of Acetonitrile/H_2O/tert-butanol=1:1:1 (v/v) and eluted with a linear gradient from B to A. Solvent A=acetonitrile, while solvent B=0.1% TFA in H_2O. Acetylated peptides were purified using a 20 min gradient from 90% to 10% B, with a yield of 30%. MTSL labeled peptides were purified using a 25 min gradient elution from 80% to 20% B, with a typical yield of 20%. Purified

peptides were lyophilized and characterized by LC-MS using a Vydac C18 analytical column with a 1 mL min^{-1} flow rate.

Circular Dichroism Spectroscopy.

CD (circular Dichroism Spectroscopy) spectra were obtained using a Jasco J-815 spectropolarimeter equipped with a peltier controlled thermostatic cell. The ellipticity is given as mean residue molar ellipticity, [θ] (10^3 deg cm^2 $dmol^{-1}$), calculated by Eqn (1).[11, 54]

$$[\theta] = (\theta_{obs} \times MRW)/(10 \times lc) \quad (1)$$

Where θ_{obs} is the ellipticity in millidegrees, MRW is the mean residue molecular weight, l is the path length of the cuvette in cm and c is the peptide concentration in mg/mL.

A 1.0 mm quartz cuvette and a final concentration of 200 μM peptide in PBS (pH=7.4). Spectra were recorded from 250 nm to 200 nm at 25 °C. Unless stated otherwise data points were collected with a 0.5 nm interval with a 1 nm bandwidth and scan speed of 1nm per second. Each spectrum was an average of 5 scans. For analysis each spectrum had the appropriate background spectrum (buffer or 50% TFE) subtracted.

For determination of the coiled coil thermal dissociation constant, temperature dependent CD spectra were obtained using an external temperature sensor immersed in the sample.[55, 56] The temperature was controlled with the internal sensor and measured with the external sensor. A 10 mm quartz cuvette was used, and the solutions were stirred at 900 rpm. Spectra were recorded from 250 nm to 200 nm, with data collected at 0.5 nm intervals with a 1 nm bandwidth and a scan speed of 1nm per second. The temperature range was 6 °C to 96 °C with a temperature gradient of 2.0 °C/minute and a 60 s delay after reaching the set temperature. The spectrum of PBS at 6 °C (average of 5 scans) was subtracted from each spectrum. All the thermal unfolding curves were analyzed using a two-state conformation transition model.[57, 58]

The data was analyzed using a two-state unfolding model to determine the fraction folded using Eqn. (2),

$$F_f = ([\theta] - [\theta]_U)/([\theta]_F - [\theta]_U) \quad (2)$$

Where [θ] is the observed molar ellipticity, $[\theta]_U$ is the ellipticity at 222 nm of the denatured state, as determined from the plateau of the ellipticity vs. temperature curve, and $[\theta]_F$ is the

ellipticity at 222 nm of the folded state at that temperature as determined from a linear fit of the initial stages of the ellipticity vs. temperature curve.

The fraction unfolded, F_U, was calculated by Eqn. (3),

$$F_U = 1 - F_f \qquad (3)$$

The dimer dissociation constant in the transition zone was calculated using Eqn. (4),

$$K_U = 2P_t F_U^2 / F_f \qquad (4)$$

P_t is the total peptide concentration. By taking the derivative of the $\ln(K_U)$ vs. Temperature and using this in the van't Hoff equation, Eqn. (5), the change in enthalpy associated with unfolding with temperature can be plotted:

$$\Delta H_U = RT^2 \times \frac{d\ln(K_U)}{dT} \qquad (5)$$

The gradient of enthalpy vs. Temperature plot ΔC_p, is the difference in heat capacity between the folded and unfolded forms, and can be used in the Gibbs-Helmholtz equation adapted to monomer-dimer equilibrium, Eqn. (6), to obtain the Gibbs free energy of unfolding as a function of temperature by least-squares fitting,

$$\Delta G_U = \Delta H_m(1 - T/T_m) + \Delta C_p[T - T_m - T\ln(T/T_m)] - RT\ln[P_t] \qquad (6)$$

T_m and H_m is the temperature and enthalpy at the midpoint of the transition at which the fraction of monomeric peptide is 0.5.[12]

^{1}H-magnetic resonance spectroscopy.

To monitor the aromatic region ^{1}H-NMR signals in the range from 8 ppm to 6 ppm of the amino acid W and Y, the proton signals of the peptide amide bonds were suppressed by proton-deuterium exchange using D_2O. Lyophilized peptide samples were dissolved at a concentration of 0.5 mg ml^{-1} and incubated in D_2O for one hour, followed by lyophilization. This procedure was repeated three times. PBS (10ml, pH=7.4) was lyophilized and redissolved in D_2O to prepare a PBS/D_2O buffer solution. Peptide samples were prepared with a final concentration of 0.8 mM in PBS/D_2O buffer solution. All ^{1}H-NMR spectra were recorded at 298 K on a Bruker Avance Ⅲ 600 MHz spectrometer with 32 scans for each sample.

Fluorescent spectroscopy.

Fluorescent experiments were conducted on a TECAN Infinite M1000 PRO fluorometer using a 96 well plate. The Z-position was 12500 μm, and the gain was optimized according to the amount of fluorophore in the sample. Excitation and emission slits were set at 5 nm. Emission spectra were measured from 290 nm to 450 nm in 1 nm steps at a fixed excitation wavelength of 275 nm. The temperature was set at 25℃. For consistent mixing, the plate was shaken inside the fluorometer for 30 seconds (2 mm linearly, 70 × per minute). The spectra were corrected by subtraction of PBS or PBS/ TFE=1:1 (v/v) spectra as a background spectrum. The concentration of peptide E or K was 20 μM in each measurement, with 250 μL volume of peptide solution in each well.

Results and discussion

Peptide design and synthesis.

In this study the feasibility to use paramagnetic NMR and fluorescence spectroscopy to investigate the orientation of the complementary peptides in a coiled coil motif was explored. For this, the well-known shortest pair of heterodimeric coiled coil scaffold Coil-K and Coil-E was used as a model system. These sequences were modified with an aromatic amino acid, either a tryptophan (W) or tyrosine (Y) at the C-terminus and the paramagnetic nitroxyl radical MTSL at selected position as the sensitive 'signal suppression' functional group (Table 1.).[16, 18, 54] A Glycine residue was added between the aromatic fluorophore and the original peptide sequence to minimize any potential influence on the coiled coil assembly. Furthermore, a cysteine residue was introduced at either the C- or N-terminus in order to label the peptide with the paramagnetic nitroxide radical via a sited-directed spin labeling (SDSL) method. MTSL was introduced via a disulfide bond to a cysteine residue as 'signal suppression' functional group.[59] The distance between the aromatic fluorophore and the nitroxide determines whether the signal is suppressed or not. Initially, MTSL was conjugated to the C-terminus of the peptide to probe the parallel assembly orientation in the coiled coil heterodimer. For comparison, the MTSL probe was placed at the N-terminus of the peptide to probe whether the antiparallel orientation would (co)exist as well (Table 1.).

All peptides which are synthesis by standard Fmoc solid phase synthesis on Rink Amide resin, and further purified by C18 RP-HPLC are characterized by both MALDI-TOF MS and LC-MS mass spectrometry. Analytical HPLC confirmed the purity of the peptide to be 99%, while UV measurements showed a purity of at least 95% (see Appendix).

Table 1. Peptide primary structure and molecular characterization.

Peptide Name	**Sequence** (from N to C terminus)	**Molecular weight** (g mol^{-1})	**^{1}H-NMR signal** [a]	**Fluorescence signal** [b]
Coil-K_W	Ac-$(KIAALKE)_3G\mathbf{W}$-$CONH_2$	2564	√	√
Coil-K_W*	Ac-$(KIAALKE)_3G\mathbf{W}C$(MTSL)-$CONH_2$	2854	×	×
Coil-*K_W	Ac-C(MTSL)$(KIAALKE)_3G\mathbf{W}$-$CONH_2$	2854	√	√
Coil-E_Y	Ac-$(EIAALEK)_3G\mathbf{Y}$-$CONH_2$	2544	√	√
Coil-E_Y*	Ac-$(EIAALEK)_3G\mathbf{Y}C$(MTSL)-$CONH_2$	2833	×	×
Coil-*E_Y	Ac-C(MTSL)$(EIAALEK)_3G\mathbf{Y}$-$CONH_2$	2833	√	√

[a]. Refers to 1D-proton NMR chemical signal for aromatic protons of tryptophan (W) and tyrosine (Y) in the range of 6-8 ppm. [b]. Refers to fluorescence emission spectra wavelength from 285-445 nm with excitation at 275 nm. Both ^{1}H-NMR and fluorescence measurements were performed in presence of pH=7.4 PBS buffer. '√' indicates there is signal observed while '×' indicates there is no signal observed.

Circular Dichroism Spectroscopy.

As single mutations in an amino acid sequence might alter the propensity to form coiled coils, the secondary structures and binding properties of all the Coil-K and Coil-E peptides including their derivatives were studied using circular dichroism (CD) spectroscopy (Figure 1 and Table 2). These results showed that in PBS buffer (pH=7.4) there is no significant change in the peptide secondary structure after introduction of the aromatic amino acids and the spin-label MTSL. All single Coil-K and Coil-E peptides retained their α-helical signature with two minimal bimodal at 222 nm and 208 nm (Fig.1A and 1B). The α-helicity and value of $[\theta]_{222}/[\theta]_{208}$ increased when the peptides were measured in 1:1 (v/v)

TFE: PBS buffer as compared to the measurements performed in PBS buffer (Table 2). This indicates that all single peptides derivatives either with or without MTSL spin label consistently kept their ability to fold in a α-helix conformation. Thus, introduction of the MTSL label does not significantly alter the secondary structure of the peptides (CD spectra of the original Coil-K ($(KIAALKE)_3$) and Coil-E ($(EIAALEK)_3$) are shown in Appendix Figure A4) .

Next, coiled coil formation of an equimolar mixture of Coil-K and Coil-E (including their MTSL derivatives) was studied, showing the typical coiled coil interactions with the helix content higher than 90% and the ratio of $[\theta]_{222}/[\theta]_{208}$ close to 1 (Figure 1C).[60, 61] Trifluoroethanol (TFE) is known to enhance the intramolecular α-helicity while disrupting intermolecular interactions.[62, 63] Addition of TFE resulted in a lower $[\theta]_{222}/[\theta]_{208}$ ratio and a decreased α-helicity confirming the existence of a coiled coil complex CC-K/E (Figure 1D).[1] CD measurements on an equimolar mixture of peptide Coil-K and peptide Coil-E with or without MTSL label showed that this modification did not significantly alter the coiled coil formation process.

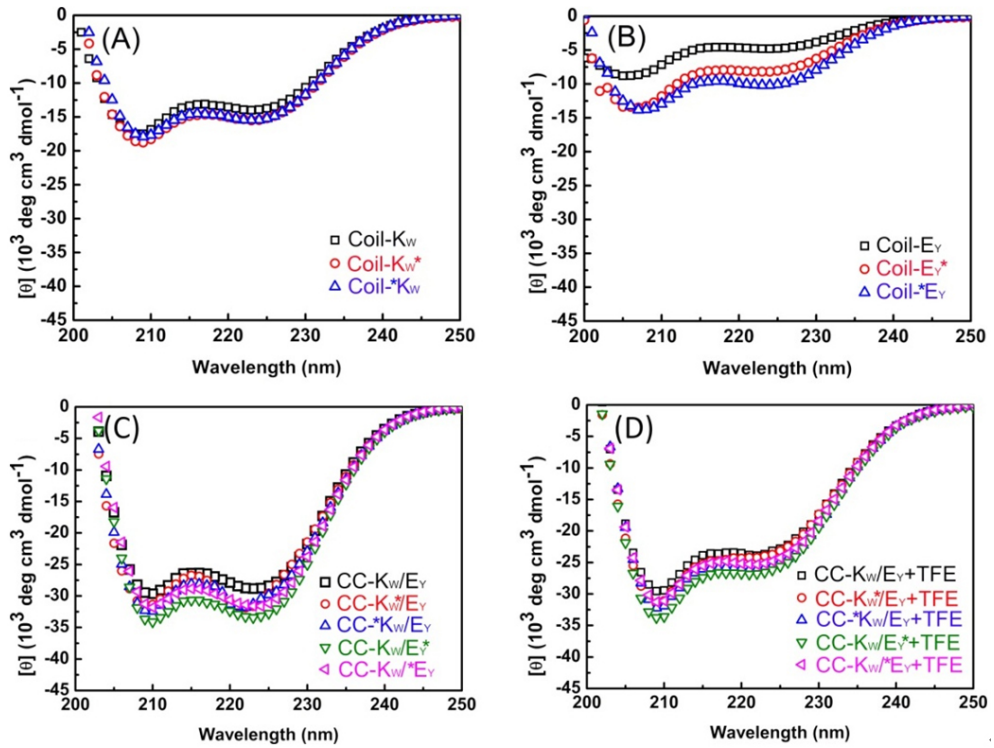

Figure 1. (A) CD spectra of secondary structure comparison of the peptides Coil-K_W, Coil-K_W^* and Coil-$^*K_W$ were measured. (B) Secondary structure comparison of CD spectra from the peptides Coil-E_Y, Coil-E_Y^* and Coil-*E. (C) Comparison of CD spectra of coiled coil motifs CC-K/E (including CC-K_W/E_Y, CC-K_W^*/E_Y, CC-$^*K_W/E_Y$, CC- K_W/E_Y^*, CC-$K_W/^*E_Y$) from an equimolar mixture of Coil-K and Coil-E peptides in pH=7.4 PBS saline. (D) Comparison of the CD spectra of the coiled coil motifs CC-K/E (including CC-K_W/E_Y, CC-K_W^*/E_Y, CC-$^*K_W/E_Y$, CC-K_W/E_Y^*, CC-$K_W/^*E_Y$) from an equimolar mixture of Coil-K and Coil-E peptides in 1:1 (v/v) PBS: TFE. [Total peptide]= 200 μM, PBS, pH=7.4, 25 ℃.

Table 2. Secondary and quaternary CD spectroscopic data of synthetic peptides used in this study.

peptide[a]	**$[\theta]_{222}$**		**% α-helix**[b]		**$[\theta]_{222}/[\theta]_{208}$**		**Coiled-coil**[c]
		50% TFE		50% TFE		50% TFE	
	PBS	In PBS	Benign	In PBS	Benign	In PBS	
Coil-K_W	-13925	-19699	43	60	0.70	0.81	-
Coil-K_W^*	-15337	-19805	46	61	0.80	0.82	-
Coil-$^*K_W$	-15411	-20057	47	61	0.81	0.82	-
Coil-E_Y	-4748	-16080	14	50	0.53	0.78	-
Coil-E_Y^*	-8180	-17727	25	54	0.61	0.78	-
Coil-$^*E_Y$	-10119	-18886	31	58	0.70	0.80	-
CC-K_W/E_Y	-28747	-23909	90	74	1.02	0.83	+
CC-K_W^*/E_Y	-31892	-24251	99	75	1.04	0.78	+
CC-$^*K_W/E_Y$	-31818	-260565	99	80	1.02	0.84	+
CC-K_W/E_Y^*	-33297	-267780	100	82	1.04	0.81	+
CC-$K_W/^*E_Y$	-31395	-25326	98	78	1.07	0.84	+

[a] CC-K/E refers to equimolar concentration mixtures of the Coil-K and Coil-E peptides. [b] The percentage of α-helicity is calculated from 100 times the ratio between observed $[\theta]_{222}$ to the predicted $[\theta]_{222}$ for an α-helical peptide of n residues. The predicted α-helicity is reckoned from formula: $[\theta]_{222}$=-4oooo×(1-4.6/n). [64, 65] [c] The signal + signifies a significant decrease in the $[\theta]_{222}/[\theta]_{208}$ ratio from benign to 50% TFE in PBS, indicative of the folded coiled-coil structure and vice versa. [Total Peptide]=200μM, PBS, pH=7.4, 25℃.

Next, the stoichiometry and binding energy of all coiled coil forming peptide pairs were determined. The binding stoichiometry of Coil-K and Coil-E mixtures was measured at a total peptide concentration of 200 μM with variable mol fractions of peptide Coil-K and Coil-E. A job-plot of $[\theta]_{222}$ as a function of the mol fraction of Coil-E peptide yields the binding stoichiometry.[66, 67] For all CC-K/E (including their MTSL derivants) coiled coil complexes studied, a minimum of $[\theta]_{222}$ was always observed at an equimolar ratio of peptide Coil-K and Coil-E, indicating that peptide Coil-K (including MTSL derivants) and peptide Coil-E (including MTSL derivants) bind in a 1:1 stoichiometry (Figure 2A). This again proves that introduction of MTSL does not interfere with the classical 1 to 1 Coil-K and Coil-E heterodimerization (Original K/E stoichiometry see Appendix, Figure A5).

The molar ellipticity at 222 nm is directly proportional to the amount of helical structure and therefore thermal denaturation curves provide information of their folding stabilities.[64, 68] Thus the thermodynamic stability of the CC-K/E pairs was determined by measuring the molar ellipticity at 222 nm wavelength as a function of temperature.[11] All peptide pairs showed a smooth cooperative transition from an α-helical coiled-coil structure to a random coil conformation (Figure 2B). All transitions showed to be fully reversible by lowering the temperature (See Appendix Figure A6).

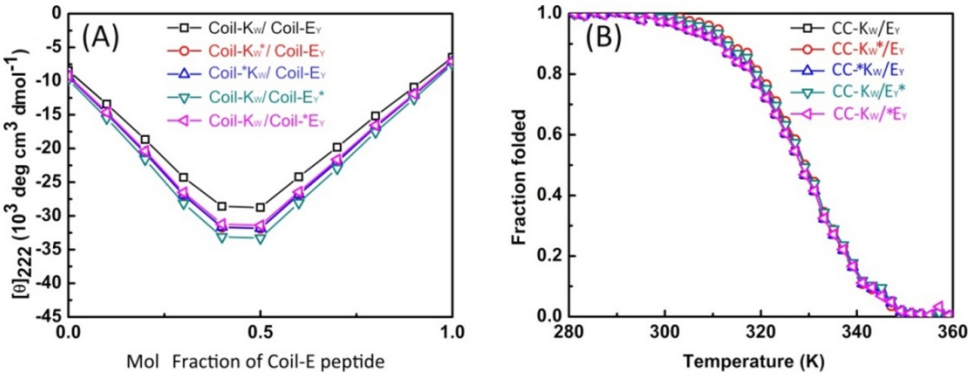

Figure 2. (A) Mean residue molar ellipticities at 222 nm wavelength for mixtures of the Coil-K and Coil-E peptides as a function of the mol fraction of the Coil-E peptide. All the measurements were carried out at a total peptide concentration of 200 μM on 25℃, in 1 mm quartz cuvette. (B) Thermal unfolding curves based on $[\theta]_{222}$ as a function of temperature. 1 cm quartz cuvette with stirring at 900 rpm was used. [Total peptide] = 40 μM, PBS, pH=7.4.

Temperature-dependent CD measurements showed that all the peptide complexes used in this study have an identical two-state transition denaturation process, dissociating from coiled coil to random coil. The binding parameters are summarized in Table 2. The dissociation constants for all coiled coils are in the same order of magnitude (10^{-8} M), showing that introduction of the MTSL residue does not influence the secondary structure, coiled coil formation and stability.

Table 3. Dissiciation constants of E and K coiled coil complex from CD spectroscopy

Coiled-coil Complex	**T_m(℃)** [b]	**ΔG_u (kcal mol^{-1})** [c]	**K_d (M)** [d]
CC-K/E[a]	58	9.6	7×10^{-8}
CC-K_W/E_Y	57	10.8	7.7×10^{-8}
CC-K_W^*/E_Y	56	11.6	6.4×10^{-8}
CC-$^*K_W$/E_Y	57	11.0	7.5×10^{-8}
CC-K_W/E_Y^*	56	11.8	6.5×10^{-8}
CC-K_W/$^*E_Y$	57	10.7	7.6×10^{-8}

[a] data taken from literature.[11, 16] [b] T_m = melting temperature, at which half of the peptide is in the unfolded form. [c] Gibbs free energy of unfolding at 25℃. [d] K_d = the dissociation constant.

^{1}H-NMR spectroscopy.

600 MHz ^{1}H-nuclear magnetic resonance spectroscopy was used to study the peptide coiled coil complex formation of peptide Coil-K and Coil-E including orientation and binding stoichiometry. Tryptophan (W) and Tyrosine (Y) residues show characteristic aromatic signals with a chemical shift in the range of 6 to 8 ppm, which in this study were used as a 'fingerprint' region in peptide Coil-K and Coil-E respectively. To avoid overlap, the N-H signals were suppressed by 'H-D exchange'. Typical NMR signals of tryptophan (W) and tyrosine (Y) in the 6-8 ppm range of peptide Coil-K and Coil-E separately are shown in (Figure 3 A/C, blue line). When a MTSL label is located close to the aromatic functional group in the same peptide, the aromatic signals are fully suppressed (Figure 3 A/C, red line), due to paramagnetic relaxation enhancement (PRE).[36, 41, 69-72] The linewidth of a proton signal will get significantly perturbed when the proton is within 13.0 Å from

the paramagnetic MTSL probe, and fully suppressed if the distance is less than 10.5 Å due to its fast transverse relaxation rate.[19,43] Theoretical calculation using Hyperchem software showed that the average distance between the MTSL nitroxide radical and the aromatic protons of the Tryptophan (W) group is 6.6 Å in Coil-K_W^* while in peptide Coil-E_Y^* the distance between MTSL and the aromatic Tyrosine (Y) group is 13.0 Å. Therefore a significant suppression of the NMR signals is observed (Figure 3 A/C, red line). In contrast, when the MTSL label is positioned on the N-terminus of the peptides, the distance between the nitroxyl radical and the tyrosine or tryptophan residues is too large in order to observe the PRE effect (Figure 3 A/C, black line). In peptide Coil-$^*K_W$, the average distance between radical and W is 36.7 Å while in peptide Coil-$^*E_Y$ the distance between radical and Y is 40.1 Å. Next, ^{1}H-NMR spectra of the individual peptides were measured in 1:1 (v/v) TFE: PBS solution to eliminate any line broadening caused by peptide aggregation and to induce maximum α-helicity.[73] In NMR experiments, peptides aggregation results in the severe NMR signals decrease and line-broadening.[18, 74-76] Even in TFE/PBS=1:1 (v/v) solution, a complete suppression of the aromatic proton was observed in Coil-K_W^* and Coil-E_Y^* confirming that the NMR signal suppression is only due to intramolecular paramagnetic relaxation enhancement (PRE) (Figure 3 B/D).

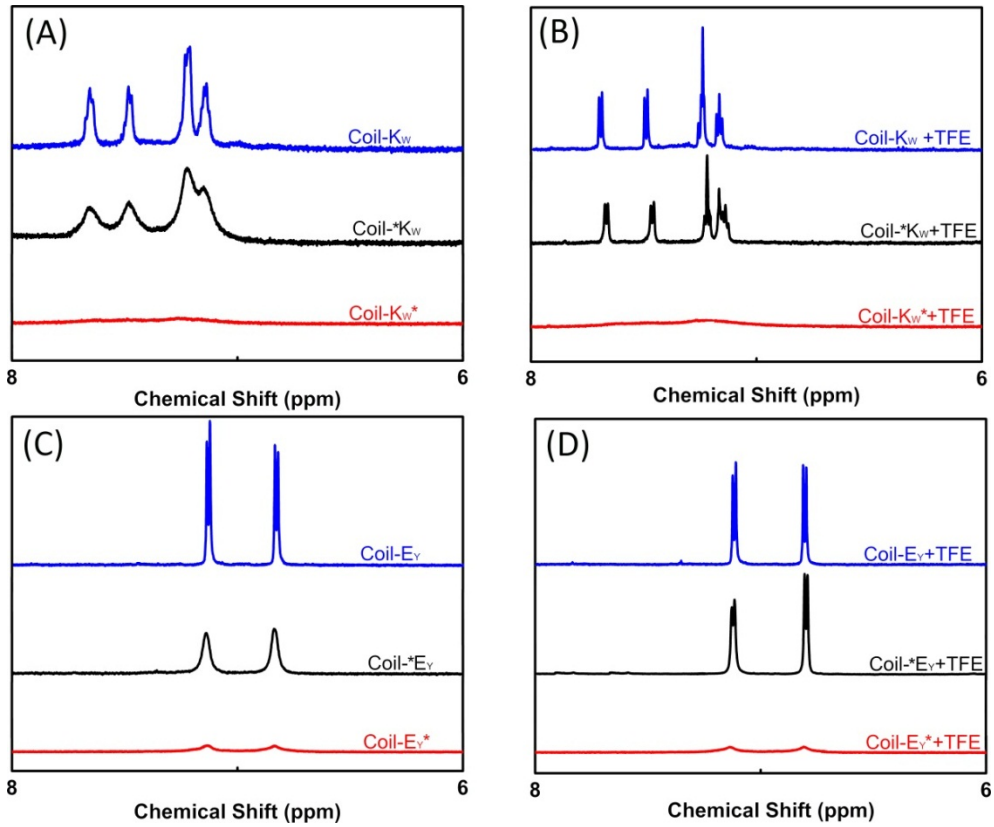

Figure 3. Aromatic region (6-8 ppm) of 600 MHz ^{1}H-nuclear magnetic resonance spectra showing tryptophan indole and tyrosine hydroxyphenyl functional groups of Coil-K and Coil-E derivatives respectively. (A) From top to bottom are the aromatic signals of Coil-K_W, Coil-$^{*}K_W$ and Coil-K_W^{*} in PBS. (B) From top to bottom are the aromatic signals of Coil-K_W, Coil-$^{*}K_W$ and Coil-K_W^{*} in 1:1 (v/v) PBS: TFE solution. (C) From top to bottom are the aromatic signals of Coil-E_Y, Coil-$^{*}E_Y$ and Coil-E_Y^{*} in PBS. (D) From top to bottom are the aromatic signals of Coil-E_Y, Coil-$^{*}E_Y$ and Coil-E_Y^{*} in 1:1 (v/v) PBS: TFE solution. [Total peptide]=0.8 mM.

Next, the coiled coil assembly of all the peptide pairs has been investigated (CC-K/E, Scheme 1). In coiled coils, complementary peptides zip together into close proximity resulting in a tight peptide complex. Therefore the PRE effect can be utilized to probe coiled coil formation and the relative orientation of the peptides within the complex.

When the MTSL label was positioned at the C-terminus of either Coil-K or Coil-E, it effectively gave suppression for both of their complementary peptides aromatic signals (Figure 4 A/C, compare blue and red trace). This indicates that peptide Coil-K and Coil-E assemble into a parallel coiled coil complex CC-K/E. In contrast, when the MTSL label

was positioned at the N- terminus, no PRE effect was observed, confirming the peptides parallel orientation (Figure 4 A/C, compare blue and black trace).

Measuring the same peptide mixtures CC-K/E in 1:1 (v/v) TFE: PBS revealed the dissociation of the coiled coil complex as observed by the reappearance of the aromatic protons of the non-MTSL labeled peptide (Figure 4 B/D).

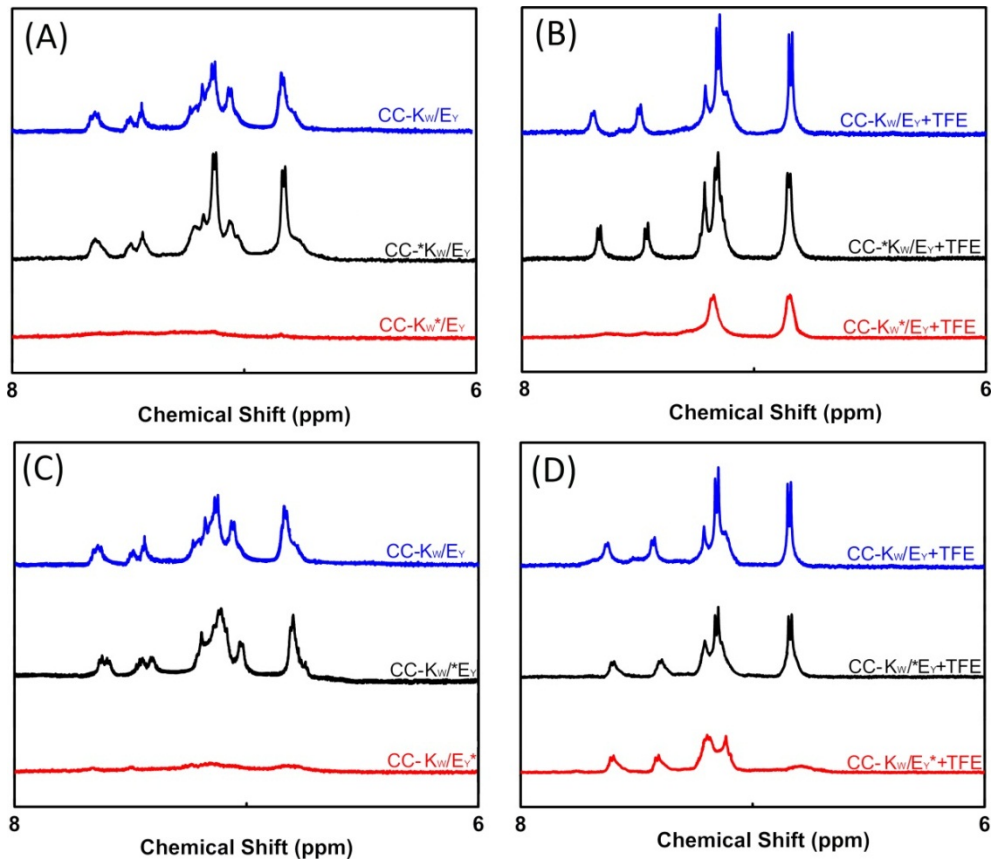

Figure 4. Aromatic Region (6-8 ppm) of 600 MHz ^{1}H-nuclear magnetic resonance spectra showing tryptophan indole and tyrosine hydroxyphenyl functional groups of equimolar mixtures of Coil-K and Coil-E (short name CC-K/E). (A) Aromatic signals of peptide CC-K/E complex in PBS. Blue line indicates CC-K_W/E_Y, black line indicates CC-$^{*}K_W/E_Y$ and red line indicates CC-$K_W{}^{*}/E_Y$. (B) Aromatic signals of CC-K/E in 1:1 (v/v) TFE: PBS. Blue line indicate CC-K_W/E_Y, black line indicates CC-$^{*}K_W/E_Y$ and red line indicates CC-$K_W{}^{*}/E_Y$. (C) Aromatic signals of CC-K/E in PBS. Blue line indicates CC-K_W/E_Y, black line indicates CC-$K_W/{}^{*}E_Y$ and red line indicates CC-$K_W/E_Y{}^{*}$. (D) Aromatic signals of CC-K/E in 1:1 (v/v) TFE: PBS. Blue line indicates Coil-K_W/E_Y, black line indicates Coil-$K_W/{}^{*}E_Y$ and red line indicates Coil-$K_W/E_Y{}^{*}$. [Total peptide]= 0.8 mM, PBS, pH=7.4.

Next, ^{1}H-NMR measurements were used to study the coiled coil binding stoichiometry. The molar ratio of Coil-K and Coil-E was varied from 2:1, 1:1 and 1:2 using peptides Coil-K_W^* and Coil-E_Y (Figure 5 A). Parallel coiled coil formation results in PRE suppression of the tyrosine residue NMR signal at the Coil-E_Y peptide as well as the tryptophan residue NMR signal at peptide Coil-K_W^*, due to their close proximity with MTSL. The measurements show that at a 2:1 and 1:1 ratio, the aromatic NMR region is silent. However, at a 1:2 ratio of peptide Coil-K_W^* and Coil-E_Y, the tyrosine signals were visible. This shows that peptides Coil-K and Coil-E indeed form a 1:1 coiled coil complex as the excess of peptide Coil-E_Y is not bound to Coil-K_W^* and thus no longer suppressed. Measuring the ^{1}H-NMR spectrum of MTSL labeled peptide Coil-E and non-labeled peptide Coil-K mixtures confirmed this finding (Figure 5B).

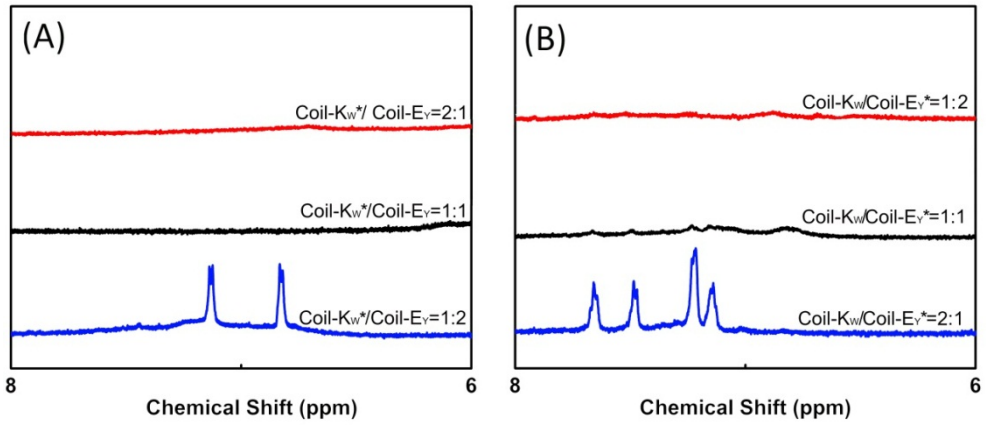

Figure 5. Aromatic region (6-8 ppm) of 600 MHz ^{1}H-nuclear magnetic resonance spectra showing tryptophan indole and tyrosine hydroxyphenyl functional groups of different molar ratio mixtures of Coil-K and Coil-E. (A) Aromatic signals of peptide Coil-K_W^* and Coil-E_Y mixtures. From top to bottom, the molar ratio between Coil-K_W^* and Coil-E_Y is 2:1, 1:1 and 1:2 respectively. (B) Aromatic signals of peptide Coil-K_W and Coil-E_Y^* mixtures. From top to bottom, the molar ratio between Coil-K_W and Coil-$^*E_Y$ is 1:2, 1:1 and 2:1. [Total peptide]=0.8 mM

Thus nitroxyl radical PRE 'signal suppression' in ^{1}H-NMR experiments is a fast and reliable method to determine the peptide folding in a coiled coil motif, showing not only the peptide orientation but also the stoichiometry.

Fluorescence spectroscopy

To support ^{1}H-NMR measurements, steady-state fluorescence spectroscopy was used to probe the orientation of peptide E and K in the coiled coils by monitoring fluorophore electron excited singlet state quenching.[48] Within a 12 Å radius, fluorescence emission quenching occurs due to electron exchange interaction between the MTSL nitroxyl radical and a tryptophan (W) or a tyrosine (Y) fluorophore.[46, 77-82] The degree of quenching is proportional to the electron exchange interaction, which is inverse proportional to the distance.[83, 84]

Excitation at a wavelength of 275 nm results in fluorescence of both tryptophan and tyrosine residues. When a MTSL group is present at the C-terminus, significant fluorescence quenching was observed for Coil-KW* and Coil-EY* (Figure 6, blue line). However, when the MTSL label is positioned at the N-terminus, the quenching is almost absent (Figure 6, red line).

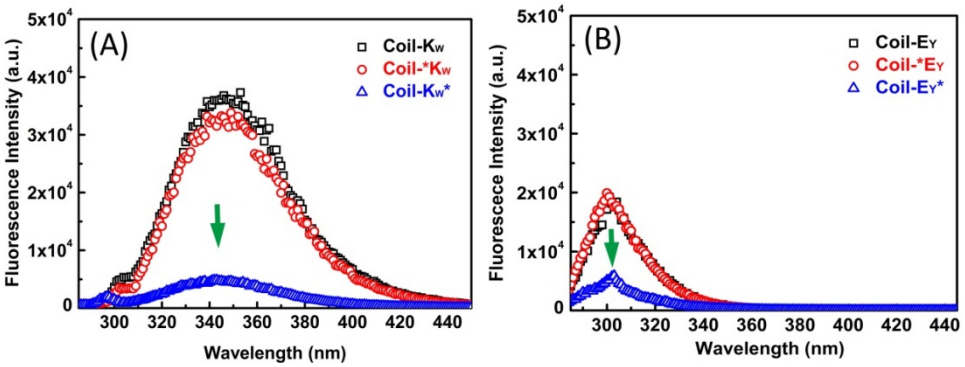

Figure 6. Fluorescence emission spectra (extension at 275 nm) of fluorescent labeled peptides Coil-K and Coil-E 50 μM in pH=7.4 PBS buffer solution on 25 ℃. (A) Presents peptide Coil-K_W (□) in black, Coil-$^{*}K_W$ (○) in red and Coil-K_W^{*} (△) in blue. (B) Presents peptide Coil-E_Y (□) in blank, Coil-$^{*}E_Y$ (○) in red and Coil-E_Y^{*} (△) in blue. Green arrow signs the fluorescence quenching position.

In the CC-K/E coiled coils both the donor fluorophore tyrosine (Y) and the acceptor fluorophore tryptophan (W) are located at the C- terminus. If peptide Coil-K_W and Coil-E_Y are adopting a parallel coiled coil orientation, the distance between W and Y is within the Förster distance ($R_0 \approx 1$ nm) resulting in fluorescence resonance energy transfer (FRET).

When the peptides assemble in an antiparallel fashion, no FRET will be observed.85 Indeed, an equimolar mixture of peptide Coil-KW and Coil-EY results in an increased fluorescence signal of acceptor tryptophan (W) and a decreased fluorescence signal of donor tyrosine (Y) due to FRET, thus indicating a parallel coiled coil orientation of peptide E and K. In the presence of TFE, the energy transfer is lost due to the dissociation of coiled coil complex (Figure 7A).

When the MTSL nitroxyl radical is close to the fluorophore on the C- terminus, the fluorophore signal will be quenched due to the electron exchange interaction (Figure 6). If the complementary peptide is close to the MTSL labeled peptide due to coiled coil formation with a parallel orientation, the signal of the complementary peptide fluorophore is also quenched (Figure 7 B/C). For example, in peptide Coil-KW*, the MTSL quenches the tryptophan signal. In an equimolar mixture of Coil-KW* and Coil-EY, the tyrosine (Y) is also quenched, indicating that the tyrosine is in the vicinity of MTSL due to coiled coil formation. This can only occur when peptide Coil-K and Coil-E assemble into a parallel heterodimer. Addition of TFE results in separation of the peptides and the tyrosine signal reappears (Figure 7B). This indicates that peptide Coil-K is close to peptide Coil-E with a parallel orientation in the coiled coil motif.

The fluorescence quenching on the other peptide pair, Coil-EY* and Coil-KW has also been studied. In this complementary coiled coil forming peptide pair, peptide Coil-EY* was labeled with both the MTSL and Tyrosine (Y) at the C- terminus. As a result, the Tyrosine emission signal was quenched. In an equimolar mixture of Coil-EY* and Coil-KW, the signal of Tryptophan (W) was significantly quenched but was recovered upon TFE addition due to the coiled coil dissociation (Figure 7C). This again proves the parallel orientation in a CC-K/E coiled coil, supporting the findings of the paramagnetic NMR studies.

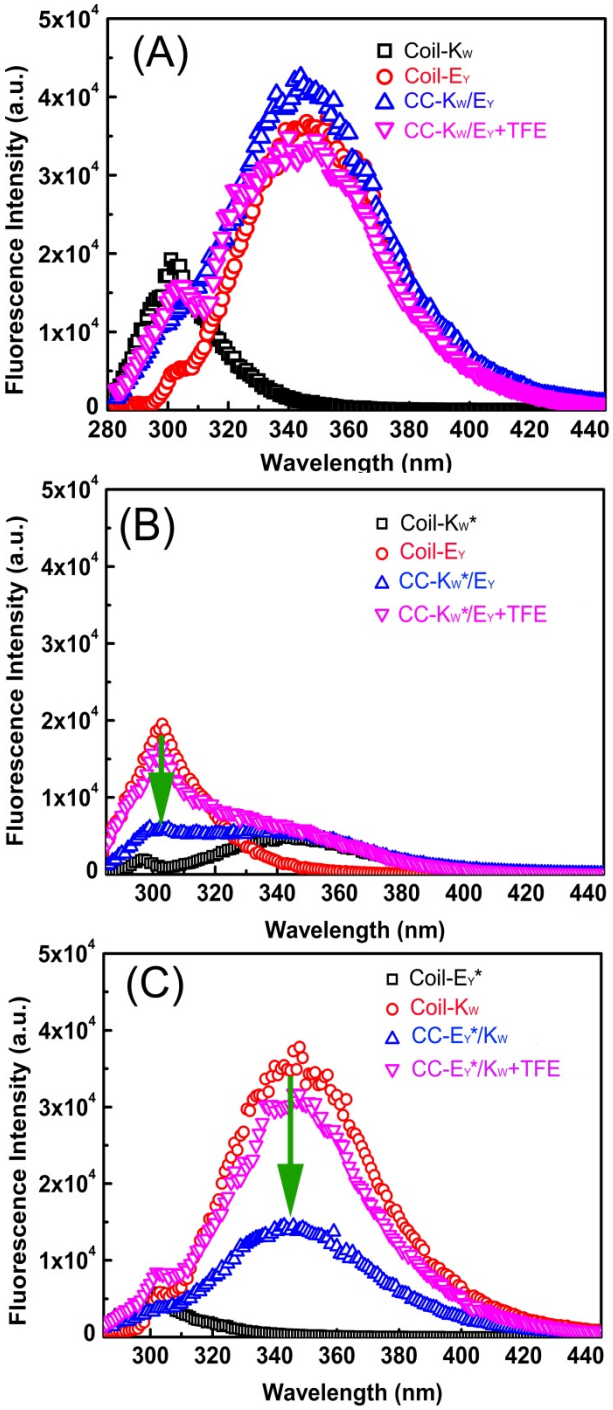
(A)
Coil-Kw
Coil-EY
CC-Kw/EY
CC-Kw/EY+TFE
Fluorescence Intensity (a.u.)
Wavelength (nm)
(B)
Coil-Kw*
Coil-EY
CC-Kw*/EY
CC-Kw*/EY+TFE
Fluorescence Intensity (a.u.)
Wavelength (nm)
(C)
Coil-EY*
Coil-Kw
CC-EY*/Kw
CC-EY*/Kw+TFE
Fluorescence Intensity (a.u.)
Wavelength (nm)

Figure 7. Fluorescence emission spectra of fluorescence labeled peptides Coil-K, Coil-E and CC-K/E (an equimolar mixture of Coil-K and Coil-E) in pH=7.4 PBS buffer solution and in 1:1 (v/v) PBS: TFE on 25℃. [Total peptide]=50 μM. (A) Presents peptide Coil-K_W (□) in black, Coil-E_Y (○) in red, CC-K_W/E_Y (△) in blue and CC-K_W/E_Y+TFE (▽) in pink. (B) Presents peptide Coil-K_W^* (□) in black, Coil-E_Y (○) in red, Coil-K_W^*/E_Y (△) in blue and Coil-K_W^*/E_Y+TFE (▽) in rosy. (C) Presents peptide Coil-E_Y^* (□) in black, Coil-K_W (○) in red, Coil-E_Y^*/K_W (△) in blue and Coil-E_Y^*/K_W+TFE (▽) in pink. Green arrow signs the fluorescence quenching position.

Conclusions

Here a new approach to investigate the supramolecular assembly of a well-known coiled coil pair, using a combination of ^{1}H-NMR and fluorescence measurements has been shown. Labeling of the peptides with Tryptophan, Tyrosine and MTSL did not influence the secondary structure of the peptides. MTSL induced suppression of specific NMR signals enables the determination of the orientation and the stoichiometry in coiled coil motifs. Fluorescence quenching by MTSL using the same peptides confirmed the finding of the NMR studies. In this study aromatic fluorophore were used as the proton signals are well-separated from the other peptide signals. In principle however, every proton signal could be used for this purpose, for example the amide signal.[41]

Comparing with the existing methods to study coiled coil assembly, this method does not require changing of the environment (e.g. Crystallization necessary for X-ray diffraction) and avoid intermolecular interaction competition between chemical bond and hydrophobic core (e.g. disulfide exchange). The field of paramagnetic NMR spectroscopy is rapidly developing, and in this contribution the use in coiled coil assembly is shown. In addition, it is compatible with two- or multi-dimensional NMR, and the same peptides can be used for EPR measurements as well for further studies.[86]

All the required manipulations are easily performed and with high efficiency. The careful choice in labeling combined with fast ^{1}H-NMR, fluorescence measurement significantly simplifies they study of non-covalent interactions in coiled coil s or other supramolecular assemblies. Further development of this approach will extensively spread on investigation of not only the peptide quaternary structure, but also most self-assembly systems.

Appendix

Part 1. Mass spectra for all the purified peptides

LC-MS spectra of all the purified peptides are shown in Figure A1.

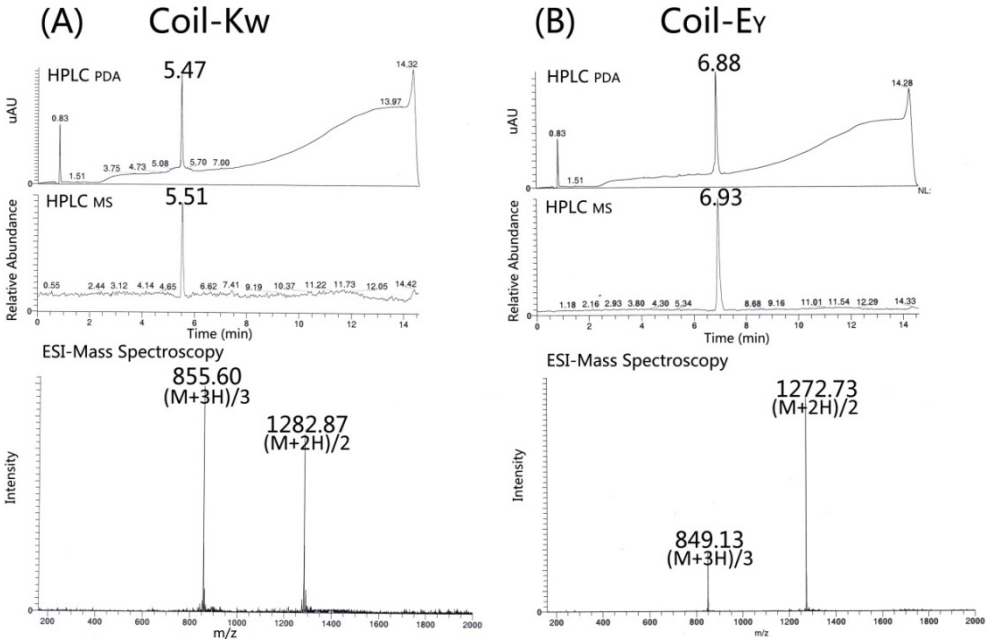

Figure A1. (A) LC-MS spectra of purified Coil-K_W, (B) LC-MS spectra of purified Coil-E_Y. From top to bottom: UV (ultraviolet-visible) spectrum, ESI (electrospray ionization) spectrum, and mass spectrum.

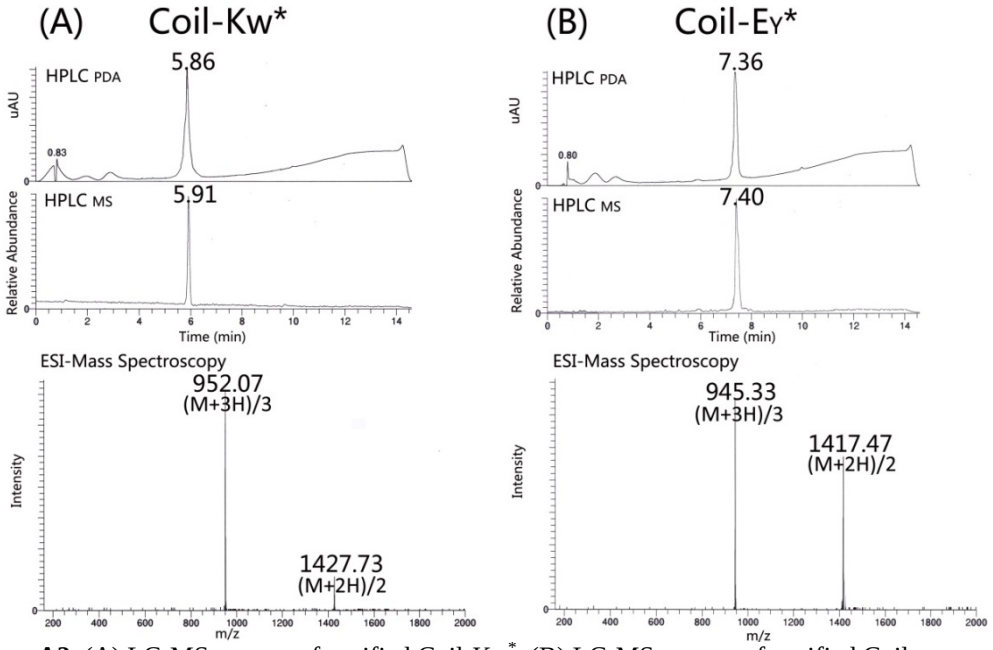

Figure A2. (A) LC-MS spectra of purified Coil-K_W^*, (B) LC-MS spectra of purified Coil-E_Y^*. From top to bottom: UV (ultraviolet-visible) spectrum, ESI (electrospray ionization) spectrum, and mass spectrum.

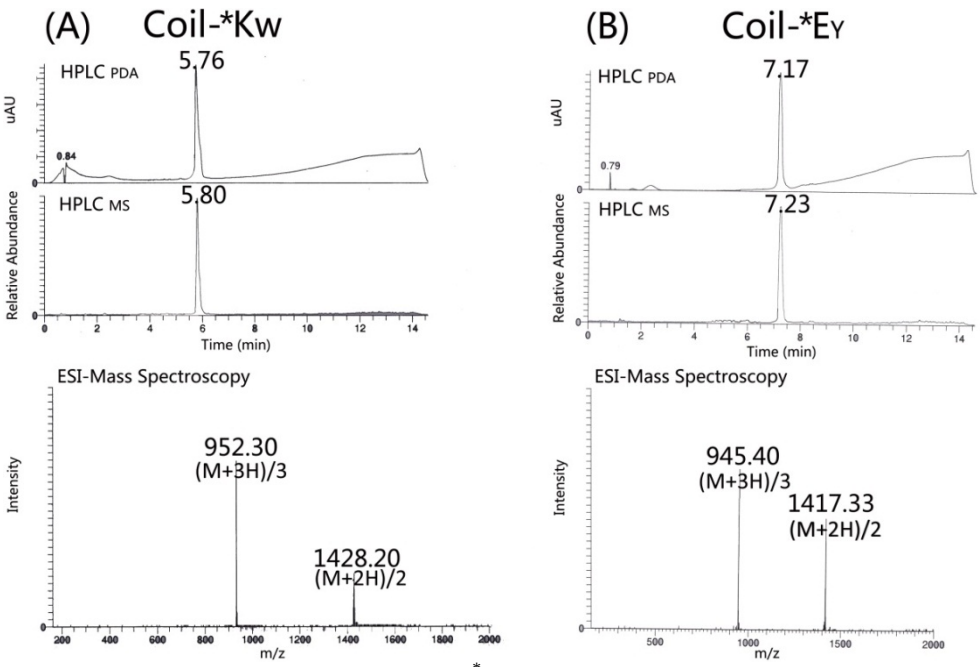

Figure A3. (A) LC-MS spectra of purified Coil-$^{*}K_{W}$, (B) LC-MS spectra of purified Coil-$^{*}E_{Y}$. From top to bottom: UV (ultraviolet-visible) spectrum, ESI (electrospray ionization) spectrum, and mass spectrum.

Part 2. CD analysis for the Hodges Coil-K and Coil-E binding.

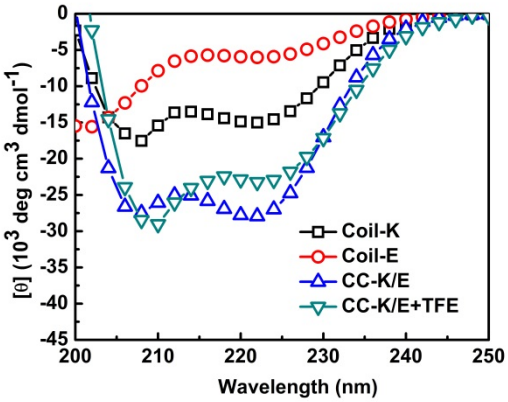

Figure A4. CD-spectra of peptide Coil-K (Ac-(KIAALKE)3-CONH2), Coil-E (Ac-$(EIAALEK)_3$-$CONH_2$), 1:1 mixture of Coil-K and Coil-E (CC-K/E) [total peptide]=200 μM in PBS (pH=7.4), 25 oC or TFE/PBS=1:1 (v/v).

Table A1. CD spectroscopic data of Coil-K, Coil-E and equimolar mixtures thereof.

Peptide [a]	θ_{222}		% α-helix [b]		$\theta_{222}/\theta_{208}$		Coiled-coil[c]
	Benign	50 % TFE	Benign	50 % TFE	Benign	50 % TFE	
Coil-K	-15010	-19788	48	63	0.86	0.92	-
Coil-E	-6016	-17067	19	55	0.6	0.78	-
CC-K/E	-27923	-23234	90	74	1.01	0.82	+

[a] CC-K/E refers to an equimolar mixture of Coil-K and Coil-E. [b] The percentage α-helicity is calculated from 100 times the ratio between observed $[\theta]_{222}$ to the predicted $[\theta]_{222}$ for an α-helical peptide of n residues. The predicted α-helicity is calculated using the formula: $[\theta]_{222}$=-40000×(1-4.6/n).[64, 65] [c] The + sign signifies a significant decrease in the $[\theta]_{222}/[\theta]_{208}$ ratio from PBS to 50% TFE in PBS, indicative of the folded coiled-coil structure and vice versa. [Total Peptide]= 200 μM in pH=7.4 PBS at 25℃.

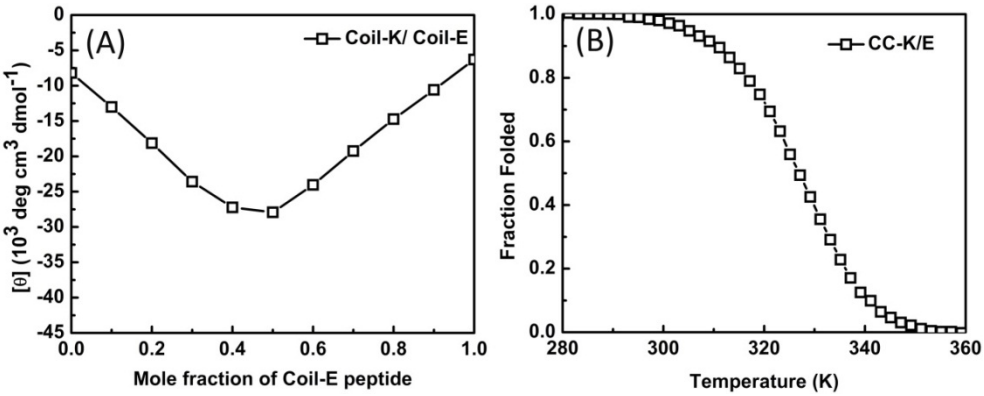

Figure A5. (A) Job plot of the mean residue molar ellipticity (222 nm) for mixtures of Coil-K and Coil-E as a function of the mole fraction of the Coil-E peptide. All the measurements were carried out at a total peptide concentration of 200 μM in pH=7.4 PBS saline buffer on 25℃, in a 1 mm quartz cuvette. (B) Thermal unfolding curve based on changes in $[\theta]_{222}$ due to dissociation of coiled coil CC-K/E. [Total peptide]=40uM, PBS, pH=7.4, 1 cm quartz cuvette.

Part 3. CD association fraction folded transitions of all coiled coils.

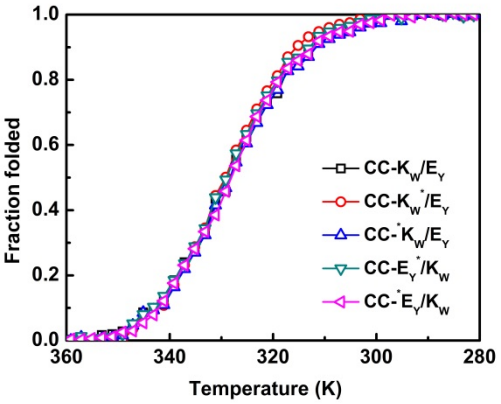

Figure A6. Thermal folding curve based on changes in $[\theta]_{222}$ as followed by CD by decreasing the temperature from 360 to 280 K. [Total peptide]=40 uM, PBS, pH 7.4, 1 cm quartz cuvette.

Part 4. Hyperchem simulations[87]

Hyperchem release 8.0 package has been used to simulate the peptide conformation and to determine the distance between MTSL and the aromatic amino acids in Coil-E and Coil-K.

For this, Coil-K, Coil-E or their 1:1 complex were placed in a periodic box containing water molecules and the system was equilibrated at 300 K. The peptide can move in a constant-density environment which is similar to being in a liquid. The size of the box was set as a cube with W=H=D= 56.104 Å, and the minimum distance between solvent and solute atoms (atoms from peptides) is 2.3 Å.88

Molecular Mechanics simulation was based on a classical Newtonian calculation. Here, atoms were treated as Newtonian particles interacting through a potential energy function, which depend on bond lengths, bond angles, torsion angles, and nonbonded interactions (including van der Waals forces, electrostatic interactions, and hydrogen bonds). In these calculations, the forces on atoms are functions of the atomic position.

Furthermore, the AMBER force field which is typically used for developing proteins and nucleic acids was used to develop an all-atom model. The simulations were performed in standard way, with temperature at 300 K and 30 ps run time.

Figures beneath shows the details of the peptide comformation zoom in to atom level after simulation. In general, Coil-K peptide secondary structure is shown in red color, Coil-E peptide secondary structure in blue color and coiled coil motif either CC-K/E or CC-E/K in

brown color. From Hyperchem simulation, information of the different distances between MTSL nitroxide radical with either proton on W or on Y have been gained as support information to the paramagnetic 1D-proton NMR spectra results (Figure A7-10).

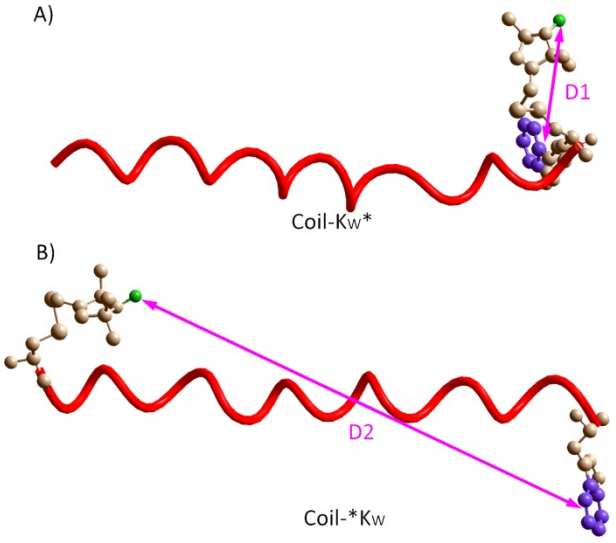

Figure A7. Structure tertiary structures of peptide Coil-KW* (A) and Coil- *KW (B). In A) D1 indicates the distance between nitroxyl group and the W in peptide Coil-KW*. The average distance D1 is 6.617 Å. In B) the average distance D2 between MTSL and W is 36.701 Å.

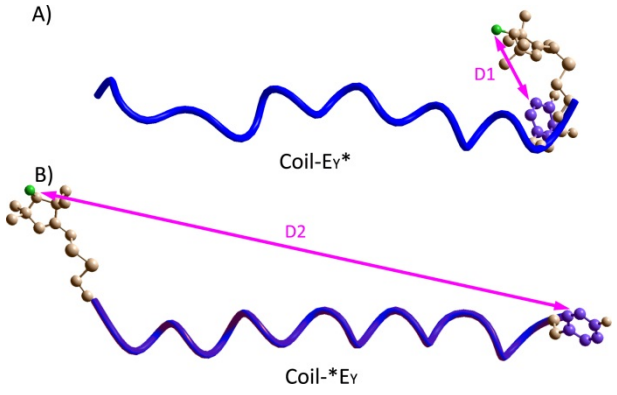

Figure A8. Structure of peptide Coil-EY* (A) and Coil- *EY (B). (A) the average distance D1= 13.0357 Å. (B) The average distance D2 = 40.0889 Å.

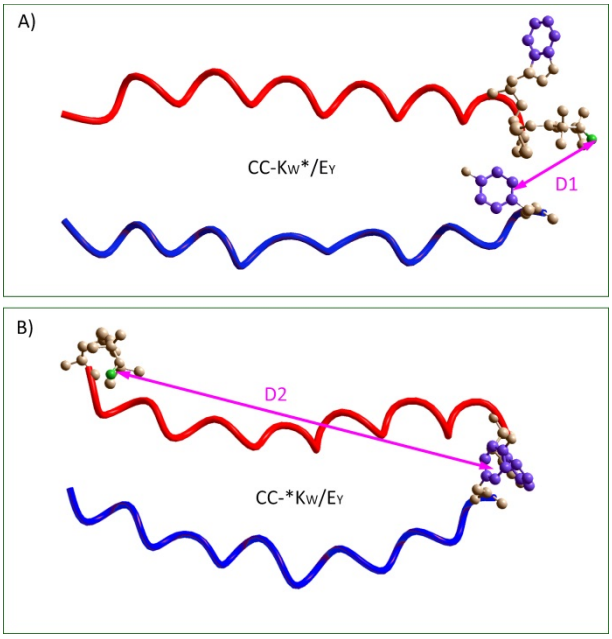

Figure A9. Coiled coil CC-K/E quaternary structure between subunits Coil-K (red) and Coil-E (blue). (A) Quaternary structure of peptide coiled coil complex CC-KW*/EY, the average distance D1=8.9315 Å. (B) Quaternary structure of CC-*KW/EY, the average distance D2=37.2628 Å.

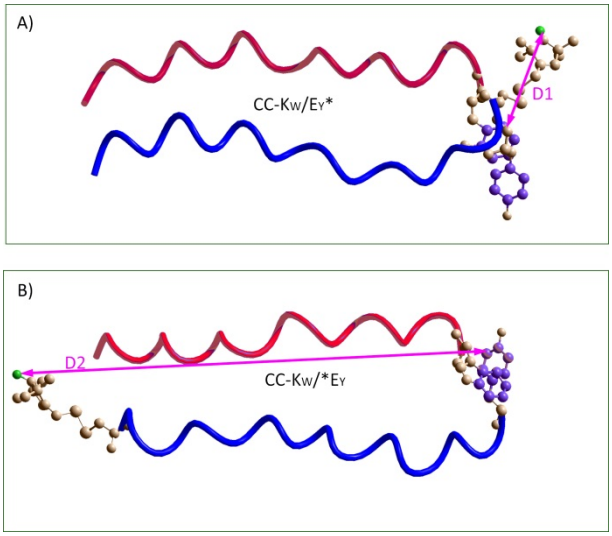

Figure A10. Coiled coil CC-K/E quaternary structure between subunits Coil-K (red) and Coil-E (blue). (A) Quaternary structure of peptide coiled coil complex CC- KW/EY*, the average distance D1=8.9315 Å. (B) Quaternary structure of CC-KW/*EY, the average

distance D2=38.7715 Å.

Part 5. The summary of the signal intensity associated with distance.

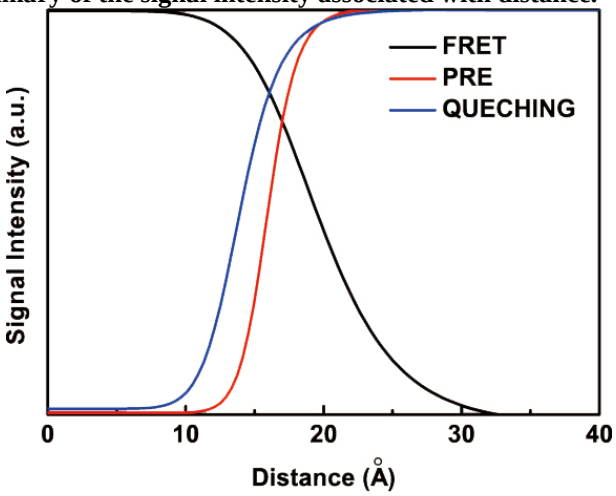

Figure A11. The distance depended signal intensity of FRET, PRE or fluorescence quenching method. The black line indicates the response distance between the FRET pair (donor and acceptor) in fluorescence resonance energy transfer (FRET) measurement; the red line indicates the response distance between the aromatic fluorophore and the MTSL nitroxyl radical in paramagnetic 1H-NMR measurement; the blue line indicates the response distance between the fluorophore and the MTSL nitroxyl radical in fluorescence quenching measurement.

Part 6. Chemical Structure of MTSL

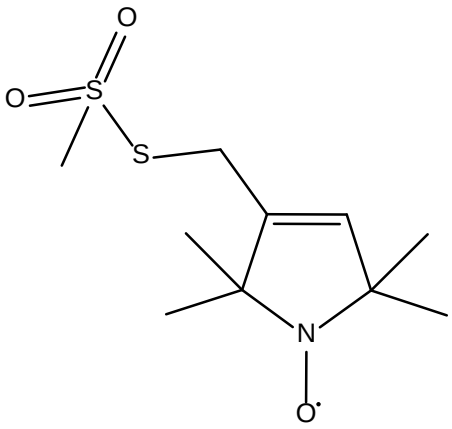

Reference

1. B. Apostolovic and H. A. Klok, *Biomacromolecules*, 2008, **9**, 3173-3180.
2. P. Burkhard, J. Stetefeld and S. V. Strelkov, *Trends in Cell Biology*, 2001, **11**, 82-88.
3. J. M. Mason and K. M. Arndt, *Chembiochem*, 2004, **5**, 170-176.
4. A. M. Slovic, J. D. Lear and W. F. DeGrado, *Journal of Peptide Research*, 2005, **65**, 312-321.
5. A. L. Boyle and D. N. Woolfson, *Chemical Society Reviews*, 2011, **40**, 4295-4306.
6. M. Spinola-Amilibia, J. Rivera, M. Ortiz-Lombardia, A. Romero, J. L. Neira and J. Bravo, *Journal of Molecular Biology*, 2011, **411**, 1114-1127.
7. J. Liu, Q. Zheng, Y. Q. Deng, C. S. Cheng, N. R. Kallenbach and M. Lu, *Proceedings of the National Academy of Sciences of the United States of America*, 2006, **103**, 15457-15462.
8. G. Grigoryan and A. E. Keating, *Current Opinion in Structural Biology*, 2008, **18**, 477-483.
9. A. Lupas, *Trends in Biochemical Sciences*, 1996, **21**, 375-382.
10. S. Takamori, M. Holt, K. Stenius, E. A. Lemke, M. Gronborg, D. Riedel, H. Urlaub, S. Schenck, B. Brugger, P. Ringler, S. A. Muller, B. Rammner, F. Grater, J. S. Hub, B. L. De Groot, G. Mieskes, Y. Moriyama, J. Klingauf, H. Grubmuller, J. Heuser, F. Wieland and R. Jahn, *Cell*, 2006, **127**, 831-846.
11. H. Robson Marsden, A. V. Korobko, T. Zheng, J. Voskuhl and A. Kros, *Biomaterials Science*, 2013.
12. T. Zheng, J. Voskuhl, F. Versluis, H. R. Zope, I. Tomatsu, H. R. Marsden and A. Kros, *Chemical Communications*, 2013, **49**, 3649-3651.
13. H. R. Marsden, N. A. Elbers, P. H. H. Bomans, N. Sommerdijk and A. Kros, *Angewandte Chemie-International Edition*, 2009, **48**, 2330-2333.
14. F. Versluis, J. Dominguez, J. Voskuhl and A. Kros, *Faraday Discussions*, 2013.
15. F. Versluis, J. Voskuhl, B. van Kolck, H. Zope, M. Bremmer, T. Albregtse and A. Kros, *Journal of the American Chemical Society*, 2013, **135**, 8057-8062.
16. J. R. Litowski and R. S. Hodges, *Journal of Biological Chemistry*, 2002, **277**, 37272-37279.
17. M. N. Oda, T. M. Forte, R. O. Ryan and J. C. Voss, *Nature Structural Biology*, 2003, **10**, 455-460.
18. D. A. Lindhout, J. R. Litowski, P. Mercier, R. S. Hodges and B. D. Sykes, *Biopolymers*, 2004, **75**, 367-375.
19. C. Landon, F. Barbault, M. Legrain, L. Menin, M. Guenneugues, V. Schott, F. Vovelle and J. L. Dimarcq, *Protein Science*, 2004, **13**, 703-713.
20. M. Huber, S. Hiller, P. Schanda, M. Ernst, A. Bockmann, R. Verel and B. H. Meier, *Chemphyschem*, 2011, **12**, 915-918.
21. D. Sheppard, C. Y. Guo and V. Tugarinov, *Journal of the American Chemical Society*, 2009, **131**, 1364-+.
22. R. P. Meadows, D. Nettesheim, R. X. Xu, E. T. Olejniczak, A. M. Petros, T. F. Holzman, J. Severin, E. Gubbins, H. Smith and S. W. Fesik, *Journal of Cellular Biochemistry*, 1993, 279-279.

23. M. Huber, A. Bockmann, S. Hiller and B. H. Meier, *Physical Chemistry Chemical Physics*, 2012, **14**, 5239-5246.
24. D. M. Engelman and P. B. Moore, *Proceedings of the National Academy of Sciences of the United States of America*, 1972, **69**, 1997-&.
25. E. K. Oshea, J. D. Klemm, P. S. Kim and T. Alber, *Science*, 1991, **254**, 539-544.
26. K. Nagai and H. Hori, *Febs Letters*, 1978, **93**, 275-277.
27. M. G. Oakley and P. S. Kim, *Biochemistry*, 1998, **37**, 12603-12610.
28. U. I. M. Gerling, E. Brandenburg, H. von Berlepsch, K. Pagel and B. Koksch, *Biomacromolecules*, 2011, **12**, 2988-2996.
29. B. Apostolovic and H. A. Klok, *Biomacromolecules*, 2010, **11**, 1891-1895.
30. B. Apostolovic, M. Danial and H. A. Klok, *Chemical Society Reviews*, 2010, **39**, 3541-3575.
31. J. Voskuhl, C. Wendeln, F. Versluis, E. C. Fritz, O. Roling, H. Zope, C. Schulz, S. Rinnen, H. F. Arlinghaus, B. J. Ravoo and A. Kros, *Angewandte Chemie-International Edition*, 2012, **51**, 12616-12620.
32. F. Versluis, J. Dominguez, J. Voskuhl and A. Kros, *Faraday Discussions*, 2013.
33. A. S. Lygina, K. Meyenberg, R. Jahn and U. Diederichsen, *Angewandte Chemie-International Edition*, 2011, **50**, 8597-8601.
34. G. Martelli, H. R. Zope, M. Brovia Capell and A. Kros, *Chemical Communications*, 2013.
35. H. Zope, C. B. Quer, P. H. H. Bomans, N. A. J. M. Sommerdijk, A. Kros and W. Jiskoot, *Advanced Healthcare Materials*, 2013, n/a-n/a.
36. L. J. Berliner, J. Grunwald, H. O. Hankovszky and K. Hideg, *Analytical Biochemistry*, 1982, **119**, 450-455.
37. G. L. Kenyon and T. W. Bruice, in *Methods in Enzymology*, eds. C. H. W. Hirs and N. T. Serge, Academic Press, 1977, vol. Volume 47, pp. 407-430.
38. I. Solomon, *Physical Review*, 1955, **99**, 559-565.
39. N. Bloembergen and L. O. Morgan, *Journal of Chemical Physics*, 1961, **34**, 842-&.
40. J. Iwahara and G. M. Clore, *Nature*, 2006, **440**, 1227-1230.
41. C. Peggion, M. Jost, W. M. De Borggraeve, M. Crisma, F. Formaggio and C. Toniolo, *Chemistry & Biodiversity*, 2007, **4**, 1256-1268.
42. K. A. Bolin, P. Hanson, S. J. Wright and G. L. Millhauser, *Journal of Magnetic Resonance*, 1998, **131**, 248-253.
43. Z. O. Shenkarev, A. S. Paramonov, T. A. Balashova, Z. A. Yakimenko, M. B. Baru, L. G. Mustaeva, J. Raap, T. V. Ovchinnikova and A. S. Arseniev, *Biochemical and Biophysical Research Communications*, 2004, **325**, 1099-1105.
44. H. E. Lindfors, P. E. de Koning, J. W. Drijfhout, B. Venezia and M. Ubbink, *Journal of Biomolecular Nmr*, 2008, **41**, 157-167.
45. S. A. Green, D. J. Simpson, G. Zhou, P. S. Ho and N. V. Blough, *Journal of the American Chemical Society*, 1990, **112**, 7337-7346.
46. N. V. Blough and D. J. Simpson, *Journal of the American Chemical Society*, 1988, **110**, 1915-1917.
47. P. L. Privalov, E. I. Tiktopulo and V. M. Tischenko, *Journal of Molecular Biology*, 1979, **127**, 203-216.

48. S. E. Herbelin and N. V. Blough, *Journal of Physical Chemistry B*, 1998, **102**, 8170-8176.
49. B. Pispisa, A. Palleschi, L. Stella, M. Venanzi and C. Toniolo, *Journal of Physical Chemistry B*, 1998, **102**, 7890-7898.
50. S. A. Palasek, Z. J. Cox and J. M. Collins, *Journal of Peptide Science*, 2007, **13**, 143-148.
51. H. Robson Marsden and A. Kros, *Angewandte Chemie (International ed. in English)*, 2010, **49**, 2988-3005.
52. T. Kaiser, G. J. Nicholson, H. J. Kohlbau and W. Voelter, *Tetrahedron Letters*, 1996, **37**, 1187-1190.
53. A. Y. Kornilova, J. F. Wishart, W. Z. Xiao, R. C. Lasey, A. Fedorova, Y. K. Shin and M. Y. Ogawa, *Journal of the American Chemical Society*, 2000, **122**, 7999-8006.
54. J. R. Litowski and R. S. Hodges, *Journal of Peptide Research*, 2001, **58**, 477-492.
55. S. M. Kelly and N. C. Price, *Biochimica Et Biophysica Acta-Protein Structure and Molecular Enzymology*, 1997, **1338**, 161-185.
56. S. M. Kelly, T. J. Jess and N. C. Price, *Biochimica Et Biophysica Acta-Proteins and Proteomics*, 2005, **1751**, 119-139.
57. P. Lavigne, M. P. Crump, S. M. Gagne, R. S. Hodges, C. M. Kay and B. D. Sykes, *Journal of Molecular Biology*, 1998, **281**, 165-181.
58. P. Lavigne, L. H. Kondejewski, M. E. Houston, F. D. Sonnichsen, B. Lix, B. D. Sykes, R. S. Hodges and C. M. Kay, *Journal of Molecular Biology*, 1995, **254**, 505-520.
59. E. J. Hustedt and A. H. Beth, *Annual Review of Biophysics and Biomolecular Structure*, 1999, **28**, 129-153.
60. N. E. Zhou, C. M. Kay and R. S. Hodges, *Biochemistry*, 1992, **31**, 5739-5746.
61. N. E. Zhou, C. M. Kay and R. S. Hodges, *Journal of Biological Chemistry*, 1992, **267**, 2664-2670.
62. N. J. Greenfield, *Nature Protocols*, 2006, **1**, 2527-2535.
63. N. J. Greenfield, *Nature Protocols*, 2006, **1**, 2876-2890.
64. Y. H. Chen, J. T. Yang and K. H. Chau, *Biochemistry*, 1974, **13**, 3350-3359.
65. N. J. Greenfield, *Nature Protocols*, 2006, **1**, 2733-2741.
66. C. Y. Huang, *Methods in Enzymology*, 1982, **87**, 509-525.
67. Z. D. Hill and P. Maccarthy, *Journal of Chemical Education*, 1986, **63**, 162-167.
68. J. A. Boice, G. R. Dieckmann, W. F. DeGrado and R. Fairman, *Biochemistry*, 1996, **35**, 14480-14485.
69. T. Gruene, M. K. Cho, I. Karyagina, H. Y. Kim, C. Grosse, K. Giller, M. Zweckstetter and S. Becker, *Journal of Biomolecular Nmr*, 2011, **49**, 111-119.
70. J. Y. Guan, P. H. J. Keizers, W. M. Liu, F. Lohr, S. P. Skinner, E. A. Heeneman, H. Schwalbe, M. Ubbink and G. Siegal, *Journal of the American Chemical Society*, 2013, **135**, 5859-5868.
71. S. Scanu, J. M. Foerster, G. M. Ullmann and M. Ubbink, *Journal of the American Chemical Society*, 2013, **135**, 7681-7692.
72. S. P. Skinner, M. Moshev, M. A. S. Hass and M. Ubbink, *Journal of Biomolecular Nmr*, 2013, **55**, 379-389.

73.J. Davies and L. Riechmann, *Febs Letters*, 1994, **339**, 285-290.
74.T. Sugiki, C. Yoshiura, Y. Kofuku, T. Ueda, I. Shimada and H. Takahashi, *Protein Science*, 2009, **18**, 1115-1120.
75.R. Page, W. Peti, I. A. Wilson, R. C. Stevens and K. Wuthrich, *Proceedings of the National Academy of Sciences of the United States of America*, 2005, **102**, 1901-1905.
76.S. Y. M. Lau, A. K. Taneja and R. S. Hodges, *Journal of Biological Chemistry*, 1984, **259**, 3253-3261.
77.F. Mito, T. Yamasaki, Y. Ito, M. Yamato, H. Mino, H. Sadasue, C. Shirahama, K. Sakai, H. Utsumi and K. Yamada, *Chemical Communications*, 2011, **47**, 5070-5072.
78.G. I. Likhtenstein, K. Ishii and S. Nakatsuji, *Photochemistry and Photobiology*, 2007, **83**, 871-881.
79.E. Gatto, G. Bocchinfuso, A. Palleschi, S. Oncea, M. De Zotti, F. Formaggio, C. Toniolo and M. Venanzi, *Chemistry & Biodiversity*, 2013, **10**, 887-903.
80.S. K. Chattopadhyay, P. K. Das and G. L. Hug, *Journal of the American Chemical Society*, 1983, **105**, 6205-6210.
81.C. V. Kumar, S. K. Chattopadhyay and P. K. Das, *Journal of the American Chemical Society*, 1983, **105**, 5143-5144.
82.W. A. Yee, V. A. Kuzmin, D. S. Kliger, G. S. Hammond and A. J. Twarowski, *Journal of the American Chemical Society*, 1979, **101**, 5104-5106.
83.J. Karpiuk and Z. R. Grabowski, *Chemical Physics Letters*, 1989, **160**, 451-456.
84.S. Atik and L. A. Singer, *Journal of the American Chemical Society*, 1978, **100**, 3234-3235.
85.J. Eisinger, *Biochemistry*, 1969, **8**, 3902-&.
86.X. Han, J. H. Bushweller, D. S. Cafiso and L. K. Tamm, *Nature Structural Biology*, 2001, **8**, 715-720.
87.I. Hypercube, 2002, 2220.